Schlichting, M., Menegazzi, P., Lelito, K., Yao, Z., Buhl, E., Dalla Benetta, E., Bahle, A., Denike, J., Hodge, J., Helfrich-Forster, C., & Shafer, O. (2016). A neural network underlying circadian entrainment and photoperiodic adjustment of sleep and activity in Drosophila. *Journal of Neuroscience*, *36*(35), 9084-9096. https://doi.org/10.1523/JNEUROSCI.0992-16.2016

A neural network underlying circadian entrainment and photoperiodic adjustment of sleep and activity in *Drosophila*.

Schlichting, M.[1*+], Menegazzi, P.[1*], Lelito, K.R.[2], Yao, Z.[2], Buhl, E.[3], Dalla Benetta, E.[1], Bahle, A.[2], Denike, J.[2], Hodge, J.J.L.[3], Helfrich-Förster, C.[1]#, and Shafer, O.T[2]#.

[1]Neurobiology and Genetics, Biocenter, University of Wuerzburg.

[2]Department of Molecular Cellular and Developmental Biology, The University of Michigan.

[3]School of Physiology and Pharmacology, University of Bristol.

[+]Current address: HHMI, Biology Department, Brandeis University

*These authors contributed equally to the manuscript.

#Correspondence to:

O.T. Shafer: oshafer@umich.edu

C. Helfrich-Förster: charlotte.foerster@biozentrum.uni-wuerzburg.de

Abstract

A sensitivity of the circadian clock to light/dark cycles ensures that biological rhythms maintain optimal phase relationships with the external day. In animals the circadian clock neuron network (CCNN) driving sleep/activity rhythms receives light input from multiple photoreceptors, but how these photoreceptors modulate CCNN components is not well understood. Here we show that the Hofbauer-Buchner eyelets differentially modulate two classes of ventral lateral neurons (LNvs) within the *Drosophila* CCNN. The eyelets antagonize Cryptochrome (CRY)- and compound-eye-based photoreception in the large LNvs, while synergizing CRY-mediated photoreception in the small LNvs. Furthermore, we show that the large LNvs interact with subsets of “evening cells” to adjust the timing of the evening peak of activity in a day-length dependent manner. Our work identifies a peptidergic connection between the large LNvs and a group of evening cells that is critical for the seasonal adjustment of circadian rhythms.

Significance Statement:

In animals, circadian clocks have evolved to orchestrate the timing of behavior and metabolism. Consistent timing requires the entrainment these clocks to the solar day, a process that is critical for an organism´s health. Light cycles are the most important external cue for the entrainment of circadian clocks and the circadian system employs multiple photoreceptors to link timekeeping to the light/dark cycle. How light information from these photorecptors is integrated into the CCNN to support entrainment is not understood. Our results establish that input from the HB-eyelets differentially impacts the physiology of neuronal subgroups. This input pathway, together with input from the compound eyes, precisely times the activity of flies under long summer days. Our results provide a mechanistic model of light transduction and integration into the circadian system, identifying new and unexpected network motifs within the CCNN.

Introduction

Circadian clocks create an endogenous sense of time that is used to produce daily rhythms in physiology and behavior (Aschoff, 1981a). A defining characteristic of a circadian clock is a modest deviation of its endogenous period from the 24.0-hour period of daily environmental change (Aschoff, 1981b). For example, the average human clock has an endogenous period of 24 hours and 11 minutes (Czeisler et al., 1999). Thus, in order to maintain a consistent phase relationship with the environment, the human clock must be sped-up by 11 minutes every day. A sensitivity of the circadian clock to environmental time cues (zeitgebers) ensures that circadian clocks are adjusted daily to match the period of environmental change (Pittendrigh, 1981). This process, called entrainment, is fundamental to the proper daily timing of behavior and physiology (Roenneberg and Merrow, 2003). For most organisms, daily light/dark (LD) cycles are the most salient zeitgeber (Aschoff, 1981b).

Though most tissues express molecular circadian clocks in animals, the clock is required in small islands of neural tissue for the presence of sleep/activity rhythms and many other daily rhythms in physiology (Herzog, 2007). Within these islands a circadian clock neuron network (CCNN) functions as the master circadian clock (Nitabach and Taghert, 2008; Welsh et al., 2010). Subsets of neurons within the CCNN receive resetting signals from photoreceptors and physiological connections between these neurons and their clock neuron targets ensure light entrainment of the CCNN as a whole (Golombek and Rosenstein, 2010).

In both mammals and insects, the CCNN receives light input from multiple photoreceptor types. In *Drosophila* the CCNN is entrained by photoreceptors in the compound eye, the ocelli, the Hofbauer-Buchner (HB) eyelets, and by subsets of clock neurons that express the blue light photoreceptor Cryptochrome (CRY) (Helfrich-Förster, 2002). Understanding how multiple light input pathways modulate the CCNN to ensure entrainment to the environmental LD cycle is critical for our understanding of the circadian system and its dysfunction when exposed to the unnatural light regimes accompanying much of modern life (Münch and Bromundt, 2012).

74 Here we investigate the physiological basis and circadian role of a long-suspected circadian
75 light input pathway in *Drosophila*: the HB-eyelets. These simple accessory eyes contain four
76 photoreceptors located at the posterior edges of the compound eyes and project directly to
77 the accessory medullae (AMe) (Hofbauer and Buchner, 1989; Helfrich-Förster et al., 2002;
78 Malpel et al., 2002), neuropils that support circadian timekeeping in insects (Helfrich-Förster,
79 1998). In *Drosophila* the AMe contain projections from ventral lateral neurons (LNvs),
80 important components of the CCNN that express the neuropeptide Pigment Dispersing
81 Factor (PDF) (Helfrich-Förster, 1997, 1998), an output required for robust circadian rhythms
82 in locomotor activity (Renn et al., 1999). The axon terminals of the HB-eyelets terminate near
83 PDF positive LNv projections (Helfrich-Förster et al., 2002; Malpel et al., 2002) and analysis
84 of visual system and *cry* mutants reveals a role for the HB-eyelet in the entrainment of
85 locomotor rhythms to LD cycles (Helfrich-Förster et al., 2001; Helfrich-Förster et al., 2002;
86 Veleri et al., 2007), but how the eyelets influence the CCNN to support light entrainment is
87 not well understood.

88 Here we present evidence that this circadian light input pathway excites the small LNvs (s-
89 LNvs) and acts to phase-dependently advance free-running rhythms in sleep/activity while
90 inhibiting the large LNvs (l-LNvs). This work reveals that input from external photoreceptors
91 differentially affects specific centers within the fly CCNN. Furthermore, we show that under
92 long summer-like days the l-LNvs act to modulate subsets of so-called evening cells to delay
93 the onset of evening activity. These results reveal a neural network underlying the
94 photoperiodic adjustment of sleep and activity.

Material and Methods

Transgenic Strains

The following fly strains were used: For GFP Reconstitution Across Synaptic Partners (GRASP): *LexAop-GFP-11*; *UAS-GFP1-10* (Gordon and Scott, 2009); *Pdf-LexA* (Shang et al., 2008); *Rh6-GAL4* (Sprecher and Desplan, 2008); *R78G02-GAL4* (Bloomington Line BL40010). For expression analysis: *UAS-cd8GFP* (Siegmund and Korge, 2001); *UAS-StingerGFP* (Barolo et al., 2000); *R78G02-GAL4* (BL40010). For live imaging experiments: *Pdf(M)-Gal4* (Renn et al., 1999); *UAS-GCaMP3.0* (Tian et al., 2009); *UAS-P2X2* (Lima and Miesenböck, 2005); *UAS-Epac1-camps(50A)* (Shafer et al., 2008); *LexAop-GCaMP3.0; LexAop-Epac1-camps* (Yao et al., 2012); *Rh6-GAL4*. For locomotor activity experiments: *UAS-TrpA1* (Hamada et al., 2008); hdc^{JK910} (Burg et al., 1993); *Rh6-GAL4*; *UAS-Kir2.1* (Baines et al., 2001); *UAS-pdfRNAi* (BL25802); han^{5304}*;UAS-PdfR* (Hyun et al., 2005; Mertens et al., 2005); *Pdf(M)-GAL4*; *R78G02-GAL4*; *R6-GAL4* (Helfrich-Förster et al., 2007); *c929-GAL4* (Hewes et al., 2000); *cry39-GAL4* (Picot et al., 2007); *Clk856-GAL4* (Gummadova et al., 2009); *Mai179-GAL4* (Grima et al., 2004); *npf-GAL4* (Lee et al., 2006); *clk4.1M-GAL4* (Zhang et al., 2010); wild-type CantonS. For electrophysiology we used a *Pdf-RFP* (Ruben et al., 2012) construct. Male flies were used for all experiments.

GRASP and Microscopy

To determine possible synapses between Rh6-cells and PDF neurons we performed GRASP experiments and processed the brains with anti-PDF. A similar approach was used to visualize putative synaptic contacts between the PDF neurons and *R78G02-GAL4* expressing neurons.

Immunocytochemistry was performed as described in Menegazzi et al. (2013). We used the following primary antibodies: mouse anti-PDF (1:1000; Developmental Studies Hybridoma Bank, The University of Iowa); chicken anti-GFP (1:2000; Abcam, Cambridge, MA); rabbit

anti-CRY (1:1000; (Yoshii et al., 2008)); guinea pig anti-VRI (1:3000; (Glossop et al., 2003)); rabbit anti-ITP (1:1000; (Hermann-Luibl et al., 2014)); mouse anti-GFP (1:1000, Sigma, St. Louis, MO). Secondary antibodies were purchased from Life Technologies (Grand Island, NY) and used in a dilution of 1:200. Brains were mounted on glass slides using Vectashield mounting medium (Vector Laboratories, Burlingame, CA).

We imaged brains using a Leica TCS SPE scanning confocal microscope (Leica, Wetzlar, Germany). We used 488, 555, and 635 nm laser diodes to excite GFP and the fluorophores of the secondary antibodies using confocal steps of 2µm. The laser settings were kept constant within each experiment. All images were analyzed using the Fiji in ImageJ.

Live Imaging

We performed live imaging experiments using an Olympus FV 1000 laser-scanning microscope (Olympus, Center Valley, PA) and a 60X 1.1N/A W, FUMFL N objective (Olympus, Center Valley, PA). We anesthetized flies over CO_2 and dissected brains under HL3 saline (Stewart et al., 1994). We mounted brains on the bottom of 35-mm FALCON culture dishes (Becton Dickenson Labware, Franklin Lakes, NJ) under a drop of HL3 saline within a Petri Dish Insert (PDI, Bioscience tools). We allowed brains to settle for 5-10 minutes before imaging. We maintained continuous HL3 perfusion while the regions of interest (ROIs) containing LNv somata or the HB-eyelet nerve were selected using Olympus Fluoview software (Olympus, Center Valley, PA). We performed Ca^{2+} imaging using the sensor GCaMP3.0, scanning brains with a 488 nm laser at 1 Hz and collecting GFP emission. We performed cAMP imaging using the FRET sensor Epac1-camps, scanning brains with a 440 nm laser at 1 Hz and collecting CFP and YFP emission. We processed GCaMP3.0 fluorescence and Epac1-camps inverse FRET (CFP/YFP) as previously described (Lelito and Shafer, 2012; Yao et al., 2012). GCaMP3.0 intensity values were filtered with a 10-point moving average. Intensity traces were then transformed to a percent fluorescence change

147 ($\Delta F/F_0$) trace using the following equation: $((F_n-F_0)/F_0)*100$, where F_n is the intensity value at
148 each point in time and F_0 is the baseline fluorescence calculated as the average
149 fluorescence intensity recorded during the first 10 seconds of imaging. Mean traces ± the
150 standard error of the mean (SEM) were created based on all GCaMP3.0 fluorescence traces
151 for each neuronal class and treatment. The maximum increase in GCaMP3.0 fluorescence
152 was determined for each filtered and normalized trace based on the entire duration of the
153 recording. These values were then used to determine the mean maximum GCaMP3.0
154 fluorescence change for each treatment and neuron type. Epac1-camps recordings
155 consisted of raw CFP and YFP values for each time-point. Spillover was corrected using the
156 following equation: YFP_{soc}= YFP-(CFP×0.444), where YFP_{soc} is the spillover corrected YFP
157 intensity, YFP and CFP are the raw intensity values, and 0.444 is the proportion of CFP
158 spillover into the YFP channel. FRET time-courses were plotted as $CFP/YFP_{soc,}$ the so-called
159 inverse FRET ratio, which proportional to cAMP levels. Inverse FRET traces were filtered
160 with a 10-point moving average and the initial time-point for each trace was normalized to
161 1.0. These filtered and normalized inverse FRET ratio traces were averaged to create
162 average traces for each treatment and neuron type and were expressed as percent changes.
163 The maximum change in inverse Epac1-camps FRET was determined for each individual
164 trace from the duration of the recording and used to generate the mean maximum changes in
165 inverse Epac1-camps FRET for each treatment and neuron type.

166 Each imaging experiment began with the acquisition of 30s of baseline fluorescence. At 30s,
167 we switched perfusion channel to a second channel, which contained either test compounds
168 dissolved in HL3 or HL3 alone as a vehicle control, for 30s, after which we switched back to
169 the first HL3 channel for the remainder of the 5-minute time-course. We purchased all
170 chemicals from Sigma-Aldrich (St. Louis, MO) and Fisher Scientific (Waltham, MA). We
171 performed statistical tests on all live imaging data using Prism 5 (GraphPad, San Diego, CA)
172 and compared maximum changes in GCaMP3.0 fluorescence or the Epac1-camps inverse
173 FRET ratio between vehicle and test compounds. We used the Mann-Whitney U test for

174 pairwise comparisons of maximum changes, and the Kruskal-Wallis one-way ANOVA with
175 Dunn's post-test for multiple comparisons. All plots were generated in Prism 5.

176

177 Analysis of Locomotor Rhythms

178 We used the Trikinetics *Drosophila* Activity Monitoring (DAM) system (Trikinetics; Waltham,
179 MA) to record the number of beam crosses caused by the fly in one-minute intervals. Flies
180 were individually placed in glass tubes containing agar-sucrose media. To address the
181 effects of HB-eyelet excitation on free running locomotor rhythms, we entrained flies
182 expressing the excitatory heat activated cation channel TrpA1 in Rh6-expressing
183 photoreceptors to a 12:12 LD cycle for 7 days at 20°C followed by constant darkness (DD).
184 We delivered a two-hour heat pulse of 30°C at ZT14 during the final night of LD and
185 continued to record locomotor activity under DD conditions for 10 days at 20°C. In order to
186 prevent signaling from Rh6 expressing photoreceptors of the compound eyes, our
187 experimental flies (*w; hdc^{JK910};Rh6-GAL4/UAS-TrpA1*) also harbored a null mutation in
188 *histidine decarboxylase,* which is required for histamine synthesis. The behavior of experimental
189 flies was compared to the behavior of *hdc^{JK910};Rh6-GAL4/+ and hdc^{JK910}; UAS-TrpA1/+*
190 controls.

191 Raw data were plotted as actograms using ActogramJ (Schmid et al., 2011). To analyze
192 phase shifts we used the open access program ChronoShop (Dr. Kamil Spoelstra,
193 Netherlands Institute of Ecology, Wageningen, Netherlands) to determine the center of
194 gravity (COG; (Diez-Noguera, 2013)) for each fly for each day of the experiment, as this is
195 the most reliable means to determine the phase of flies lacking input from the compound
196 eyes (Rieger et al., 2003). To determine the COG under entrained conditions, we averaged
197 the COG of the last 2 days in LD. To determine the phase shift induced by the heat pulse, we
198 calculated the difference between COG on day 1 (COG1) after the heat pulse and COG in
199 entrained conditions. The same was done for day 2 after the heat pulse (COG2). To

compensate for differences in the free-running period, we subtracted the shift caused by the free-running period at COG1 and COG2 for each single fly. We calculated the shift caused by the heat pulse as the mean of ΔCOG1 and ΔCOG2. The free-running period was analyzed using chi2 analysis.

For the determination of the evening peak timing under long days we entrained flies for eight days under LDR 16:8 (a light/dark cycle with 1.5 hours gradual increase or decrease in light intensity after lights-on or before lights-off, respectively). Only the final five days of locomotor activity were used in our analysis. Average activity recorded from day three to eight was plotted for each fly and the average evening peak time scored as previously described (Schlichting and Helfrich-Förster, 2015). Statistical analysis was performed using ANOVA with a Tukey's multiple comparison test for normally distributed data and the Kruskal-Wallis test with a Dunn's multiple comparisons test for non-normally distributed data. In both cases p values were adjusted using a Bonferroni correction.

Electrophysiology

We visualized the l-LNvs flies containing the RFP-tagged construct *Pdf-RFP* (*yw;Pdf-RFP*) using a 555 nm LED light, the use of which prevented the excitation of CRY. Adult flies raised under a 12h:12h LD cycle at 25°C, were collected ~3-5 days post eclosion between ZT 1 and 3, where ZT0 corresponds to lights-on. Flies were decapitated and brains dissected in extracellular saline solution containing (in mM): 101 NaCl, 1 $CaCl_2$, 4 $MgCl_2$, 3 KCl, 5 glucose, 1.25 NaH2PO4, 20.7 $NaHCO_3$, with pH adjusted to 7.2 (Cao and Nitabach, 2008). We transferred dissected brains to saline containing 20 U/ml papain with 1 mM L-cysteine for three minutes to digest the ganglion sheath. We then dissected away the photoreceptors, air sacks and trachea, and made a small incision over the position of the l-LNv. Brains were placed ventral side up in the recording chamber, secured using a custom-made anchor (Chen et al. 2015). We perfused brains continuously with aerated (95% O_2, 5% CO_2) saline

solution. We identified l-LNvs on the basis of their RFP fluorescence, size and position. We performed a single whole cell current clamp recording from one l-LNv per brain using glass electrodes with 10-20 MΩ resistance filled with intracellular solution (in mM: 102 K-gluconate, 17 NaCl, 0.94 EGTA, 8.5 HEPES, 0.085 $CaCl_2$, 1.7 $MgCl_2$, pH 7.2). Recordings were made using an Axon MultiClamp 700B amplifier, digitized with an Axon DigiData 1440A (sampling rate: 20 kHz; filter: Bessel 10 kHz), and recorded using pClamp 10 (Molecular Devices, CA, USA). An l-LNv was included in the analysis if the access resistance was less than 70 MΩ and the leak current in response to a -40 mV pulse less than -100 pA. Histamine (100 mM) was injected in the ipsilateral medulla via a glass pipette (1-3 MΩ) and a Picospritzer III (5-10 PSI; Parker Hannifin, NH, USA). All chemicals were purchased from Sigma (Poole, UK). The liquid junction potential was calculated as 13 mV and was subtracted from all the membrane voltages.

Results:

The Rhodopsin-6 photoreceptor termini rest in close apposition to the LNvs in the accessory medulla but not in the distal medulla.

In order to express transgenes in the HB-eyelets, we made use of the *Rh6-GAL4* driver, as the eyelets express Rhodopsin-6 strongly in the adult (Helfrich-Förster et al., 2002). The R8 photoreceptors of the compound eyes are also targeted by *Rh6-GAL4* (Yasuyama and Meinertzhagen, 1999) and we are not aware of a driver that drives strong expression exclusively in the HB-eyelets. R8 photoreceptors terminate in the distal medulla of the optic lobes whereas the eyelets project to the AMe where they terminate near the LNvs and along the ventral elongation of the AMe (Helfrich-Förster et al., 2002; Malpel et al., 2002) and Figures 1A-F). If synaptic connections exist between the Rh6-expressing photoreceptors (Rh6-PRs) and the LNvs, split GFP constructs driven independently in these cell types should result in the reconstitution of GFP (Feinberg et al., 2008), whereas a lack of reconstitution would argue against the presence of direct connections between these photoreceptors and the LNvs. Expression of split GFP in Rh6-PRs and LNvs resulted in the reconstitution of GFP specifically in the AMe in 16 of 16 brains imaged. In 13 of these brains we observed GFP reconstitution along the previously described ventral elongation of the LNv projections ((Helfrich-Förster et al., 2002; Helfrich-Förster et al., 2007); Figures 1G-L). No GFP reconstitution was detected in other regions of the brain, not even in the distal medulla where R8 termini reside near projections of the large LNvs (l-LNvs). We detected no GFP fluorescence in control parental genotypes containing either the genetic drivers alone or the split GFP elements without drivers (Figures 1G and 1I). These results support the hypothesis that the eyelets form direct connections on the LNvs in the AMe and its ventral elongation.

Excitation of Rhodopsin-6 expressing photoreceptors causes Ca^{2+} and cAMP increases in the small but not the large LNvs and shifts free-running locomotor rhythms.

In the adult fly, the HB-eyelets are immunoreactive to antisera raised against both, choline acetyl transferase (ChAT) and histamine (Pollack and Hofbauer, 1991; Yasuyama and Salvaterra, 1999), suggesting the presence of acetylcholine and histamine in the eyelet nerves. It is not known if the eyelets employ both neurotransmitters in the adult or if anti-ChAT immuno-signals represent a waning pool of ChAT left over from Bolwig's nerves, which is remodeled to become the eyelets (Helfrich-Förster et al., 2002; Malpel et al., 2002). It is not known if either neurotransmitter is used to relay light information from the eyelets to the clock neurons in the AMe, though previous work established that both the l-LNvs and s-LNvs are receptive to acetylcholine (McCarthy et al., 2011; Lelito and Shafer, 2012).

To determine if an excitatory connection exists between the Rh6-PRs and the LNvs, we rendered the HB-eyelet nerves excitable by ATP through the expression of the mammalian purinergic receptor P2X2 (Lima and Miesenböck, 2005); via *Rh6-GAL4* mediated expression of UAS-P2X2 (Figure 2A). When we excited Rh6-PRs no Ca^{2+} responses were detected in the l-LNvs (Figure 2B). In contrast, the s-LNvs displayed significant Ca^{2+} increases (Figure 2C). This excitatory response was not due to non-specific effects of ATP or to leaky P2X2 expression in the small LNvs, as ATP perfusion in flies lacking the *Rh6-GAL4* driver for the directed expression of UAS-P2X2 did not result in s-LNv Ca^{2+} increases (Figure 2D). In fact, in this case ATP perfusion caused the maximum GCaMP fluorescence changes to be negative in the s-LN_vs (Figure 2D), The s-LNvs consistently express lower sensor levels than the l-LNvs, this tendency is accompanied by relatively high sensitivity to movement artifacts, non-specific effects of bath applied compounds, and bleaching during imaging experiments, thus the excitatory response we measure for the s-LNvs in response to Rh6 PR excitation (Figure 2C) may underestimate the s-LNv response magnitude.

These results suggest that the HB-eyelets provide excitatory drive to the s-LNvs but not the l-LNvs. The presence of anti-ChAT immunosignals in the eyelet nerve (Yasuyama and Meinertzhagen, 1999) suggests that acetylcholine mediates this excitation. Cholinergic agonists increase cAMP levels in both the l-LNvs and s-LNvs (Lelito and Shafer, 2012).

Thus, if the eyelets excite the s-LNvs but not the l-LNvs, excitation of the eyelets should cause cAMP increases in the former but not the latter neuron class. Indeed, excitation of Rh6-PRs produced no significant cAMP changes in the l-LNvs (Figure 2E) but caused clear increases in cAMP in the s-LNvs (Figure 2F). Neither the l-LNvs nor s-LNvs displayed cAMP increases in the absence of the GAL4 driver for P2X2 expression (Figures 2G and 2H). These results suggest that among the LNvs the HB-eyelet specifically excites the s-LNvs.

The acute excitation of LNvs results in phase dependent advances and delays in free-running locomotor rhythms (Guo et al., 2014). Thus, an excitatory connection between the HB-eyelets and the s-LNvs leads to the predication that eyelet excitation will result in phase shifts in the fly's rhythm. We therefore expressed the heat activated cation channel TrpA1 (Hamada et al., 2008) in the R6-PRs by combining *UAS-TrpA1* with *Rh6-GAL4*, thereby rendering the R6-PRs excitable by high temperature (30°C) pulses. Because a previous study has shown that signals from the compound eyes increase the neuronal firing rate of the l-LNvs (Muraro and Ceriani, 2015), we conducted this experiment in a null hdc^{JK910} mutant, which is unable to synthesize histamine (Burg et al., 1993). In this way TrpA1 mediated excitation of Rh6-PRs should result in acetylcholine release from the HB-eyelets in the absence of histamine release from the R8 photoreceptors in the compound eye or HB-eyelets.

At low temperature (20°C), the expression of TrpA1 in the Rh6-PRs of hdc^{JK910} mutants caused a significant decrease in the free-running period of locomotor rhythms relative to controls (EXP: 23.5 ± 0.1; GAL4: 24.3 ± 0.1; UAS: 24.3 ± 0.1). Although dTrpA1 channels are gated by temperatures above ~25 °C (Viswanath et al., 2003) and temperatures above 25 °C have been observed to provoke measurable behavioral changes when dTrpA1 is overexpressed in neurons of interest (reviewed in Bernstein et al., 2012), we cannot exclude the possibility that some dTrpA1 mediated currents where present at 20°C in Rh6 photoreceptors overexpressing dTrpA1. Slight depolarization due to such currents could be the cause of the slight period shortening we observed in our experimental flies. We were

unable to measure the free-running period of these flies at high temperature due to low survivorship. We excited the Rh6 expressing photoreceptors of experimental flies at ZT 14 with a two-hour pulse of high temperature, comparing the phase responses of experimental flies to the heat pulse to those of genetic controls that lacked either *Rh6-GAL4* or *UAS-TrpA1* elements. The heat pulse resulted in a small but significant ($p<0.001$) phase advance of the free-running behavior in the experimental line (88 ± 14 min) compared to both controls (GAL4: -3 ± 15 min; UAS: 4 ± 13 min). A phase advance at this time was surprising, given previous work indicating that the excitation of the large and small LNvs at ZT 15 cause phase delays (Guo et al., 2014). However, recent work has revealed that the specific excitation of the s-LNvs causes only advances in the free-running locomotor rhythm and that LNv induced delays requires the excitation of the l-LNvs (Eck at al. 2016). Thus, HB-eyelet excitation modestly but significantly shifted the phase of free running locomotor rhythms during the early night in a manner consistent with the specific excitation of the s-LNvs.

Histamine inhibits the large LNvs, which govern evening peak phase under long days.

Given the effect of cholinergic input into the CCNN, we wondered whether histamine release from the eyelets can elicit changes in Ca^{2+} and/or cAMP. Mapping of the inhibitory histamine receptor HisCl indicated that the large but not the small LNvs are receptive to histamine (Hong et al., 2006). We found no evidence that bath-applied histamine caused significant changes in Ca^{2+} or cAMP in either the l-LNvs or s-LNvs using live imaging methods (data not shown). Histamine acts through inhibitory receptors (Pantazis et al., 2008) and inhibition is often difficult to detect with Ca^{2+} and cAMP sensors (Lelito and Shafer, 2012), suggesting that histamine either does not inhibit the LNvs or that such inhibition is not detectable with genetically encoded sensors.

Despite our inability to measure histamine responses in the l-LNvs using genetically encoded sensors, the HB-eyelet's immunoreactivity to histamine (Pollack and Hofbauer, 1991), the

expression of the inhibitory histamine receptor HisCl by the l-LNvs (Hong et al., 2006), and the GRASP results reported above, together suggest that the eyelets act to inhibit the l-LNvs. We therefore performed electrophysiological recordings and asked if histamine had inhibitory effects on the l-LNvs that were not detectable using our live imaging methods. The l-LNvs are characterized by spontaneous firing (Sheeba et al., 2008). Local application of 100mM histamine reliably stopped spontaneous spiking of the l-LNvs (n = 5) in a manner dependent on the duration of histamine application (Figure 2I,J). In three out of five recordings, histaminergic inhibition of the l-LNvs revealed persistent but much smaller spikes that likely originated from the contralateral l-LNv arbor as previously reported (Cao and Nitabach, 2008). These results suggest that histamine exerts its inhibitory effects locally and briefly, specifically within the hemisphere of histamine application. Though this is consistent with a histaminergic connection between the eyelets and the l-LNvs, we note here that are other potential sources histamine in the AMe (Hamasaka and Nässel, 2006).

Given the modulatory effect of histamine on the l-LNvs, we wondered whether changing the properties of these neurons might affect the behavior of flies. Flies lacking PDF peptide or LNvs display abnormally advanced peaks of evening activity (Renn et al., 1999). Previous work suggested that PDF from either the l-LNvs or the s-LNvs is sufficient for the normal timing of the evening peak under equinox (Shafer and Taghert, 2009) suggesting that PDF released from the l-LNvs, though not required for normal evening peak phase, nevertheless contributes to evening peak timing. We asked if PDF released from the l-LNvs might be required for normally timed evening peak phase under long day conditions. As previously shown for equinox, the knockdown of PDF from all LNvs resulted in a significant advance in the evening peak of activity (Figures 3A, 3B, and 3F) in a manner reminiscent of the loss of PDF neuron function (Figure 3E). In contrast to previous experiments under LD 12:12, knockdown of PDF specifically in the l-LNvs resulted in a significant advance in the evening peak under long days (Figures 3C, 3E, and 3G), whereas the knockdown of PDF specifically in the s-LNvs had no obvious effects on the evening peak compared to controls under long day conditions (Figures 3D, 3E, and 3H). The knockdown of PDF in both the l-LNvs and s-

LNvs produced a larger effect on the evening phase than the knockdown in the l-LNvs alone (Figures 3B, 3C, and 3E). This difference is likely a reflection of differing levels of GAL4 mediated RNAi expression by *Pdf-GAL4* and *c929-GAL4*.

Excitation of the l-LNvs produces Pigment-dispersing factor receptor-dependent cAMP increases in the s-LNvs.

The finding that PDF is required specifically in the l-LNvs for the normal phasing of the evening peak of activity under long days suggested that these neurons, previously characterized as wake promoting neurons with limited control over circadian timekeeping (Parisky et al. 2008; Chung et al. 2008; Shang et al., 2008; Sheeba et al., 2008), might modulate the evening cells of the CCNN, either directly or indirectly through actions on the s-LNvs. Anatomical evidence suggests that the large LNvs might modulate the critical s-LNv pacemakers: projections from the l-LNvs reside in close apposition to s-LNv dendrites (Helfrich-Förster et al., 2007) and the s-LNvs are receptive to PDF (Shafer et al., 2008; Im and Taghert, 2010). The excitation of the *c929-GAL4* positive neurons, which include the l-LNvs, does not produce excitatory Ca^{2+} responses in the s-LNvs (Yao et al., 2012). Given that the PDF receptor signals predominantly through increases in cAMP (Hyun et al. 2005; Mertens et al. 2005; Shafer et al. 2008), we asked if the s-LNvs responded to the excitation of the l-LNvs with cAMP increases by expressing the P2X2 receptor in the *c929-GAL4* positive neurons of the brain while simultaneously expressing the cAMP sensor Epac1-camps in the l-LNvs and s-LNvs. As expected ATP mediated excitation of the *c929*-positive network in *c929-GAL4/Pdf-LexA*, *LexAop-Epac-1camps;UAS-P2X2*/+ brains resulted in excitatory cAMP responses in the l-LNvs (Figures 4A and 4G). Excitation of the l-LNvs was accompanied by cAMP increases in the s-LNvs (Figures 4B and 4H.) suggesting the presence of a modulatory connection between *c929* positive neurons and the s-LNvs.

While *c929-GAL4* is expressed in the l-LNvs but not the s-LNvs, it is also expressed in many other peptidergic neurons of the CNS (Hewes et al., 2003). To determine if the l-LNvs were responsible for the cAMP response in the s-LNvs we repeated the *c929-GAL4* excitation experiment in a loss of function PdfR mutant (han^{5304}) background. Perfusion of ATP caused excitatory cAMP responses in the l-LNvs of han^{5304}*;c929-GAL4/Pdf-LexA, LexAop-Epac-1camps;UAS-P2X2/+* brains (Figures 4C and 4G.) but failed to produce significant cAMP increases in the s-LNvs (Figures 4D and 4H), suggesting that PDF released from the l-LNvs was responsible for the effects of *c929* network excitation on the s-LNvs. Flies expressing cAMP sensor in the LNvs that contained the *UAS-P2X2* element but lacked the *c929-GAL4* driver displayed no responses to bath applied ATP in either the l-LNvs or the s-LNvs (Figures 4E-4H) indicating that the excitatory responses in the l-LNvs in the previous experiments were indeed due to the specific expression of P2X2 in the *c929* network. These results reveal a modulatory connection from the l-LNvs to the s-LNvs and indicate that PDF released from the former neurons accounts, at least in part, for the activation of PDF receptor in the s-LNvs.

Expression of PdfR in four evening cells is sufficient for the normal phase of evening activity under long days.

Given the presence of a modulatory connection between the large and small LNvs, the l-LNvs might influence the phase of the evening peak by modulating the clock within the s-LNvs. (We note here that PDF is not the only transmitter produced by the s-LNvs and that these neurons are anatomically well-suited to modulate most components of the CCNN.) Like pdf^{01} mutants and flies with reduced PDF in the l-LNvs, loss of function *pdfr* mutants display an abnormally advanced evening peak (Hyun et al., 2005). This was also clear in *pdfr* mutants observed under LDR 16:8 (Figures 5A and 5F). If the l-LNvs adjust the evening peak of activity through the modulation of the s-LNvs, then we would predict that *pdfr* would be required in the s-LNvs for normal evening peak phase under LDR 16:8. Rescue of *pdfr*

expression in the LNvs (*Pdf-GAL4*) or specifically in the s-LNvs (*r6-GAL4*) of *han*^{5304} mutants failed to produce a normally phased evening activity peak relative to *han*^{5304}*;UAS-pdfr* controls (Figures 5B and 5F). This result is not surprising given that *pdfr* is likely required in evening cells for the reception of PDF from either class of LNv. In order to challenge this idea we rescued *pdfr* expression within the evening cells via the *R78G02*-GAL4 driver, which is expressed in the 5th s-LNv and the three *cry* expressing LNds, in addition to approximately fifteen neurons outside of the clock network (Figures 5G, 5H). In these flies the evening activity peak displayed a delayed phase compared to *pdfr*$^{-}$ controls (Figures 5D and 5F). To confirm this finding we rescued *pdfr* expression with several other *GAL4* drivers. Expression of *pdfr* with all driver lines including these neurons (*Clk856*-GAL4, *cry39-GAL4 and Mai179-GAL4*) rescued the phase of the evening peak (Figures 5C and 5F). Conversely, the expression of *pdfr* using the *Clk4.1M-GAL4*, a driver expressed only in the DN1p class of clock neurons, failed to rescue the phenotype (Figure 5F).

Taken together, our *pdfr* rescue results suggest that *pdfr* expression within the 5th s-LNv and a subset of the LNds is sufficient for normal evening peak phase under long days. When used in conjunction with *Pdf-LexA*, GRASP experiments with *R78G02-GAL4* revealed the reconstitution of GFP within the AMe and along the dorsal projection of the s-LNvs (Figures 5I and 5J), consistent with synaptic connections between the LNvs and the *R78G02-GAL4* positive network. Neuropeptide F (NPF) is expressed by the 5th s-LNv and is also expressed in one *R78G02-GAL4* positive LNd in each hemisphere. These neurons also express Ion Transport Peptide (ITP; (Johard et al., 2009)). Rescue of *pdfr* expression using *npf-GAL4* almost completely rescued the evening peak phase (Figures 5E and 5F) revealing that *pdfr* expression in the NPF/ITP positive LNd and 5th s-LNv is largely sufficient for the normal phasing of the evening peak under long days. This indicates that the *pdfr* dependent modulatory connection between the l-LNvs and the s-LNvs is not required for the adjustment of the evening peak by the l-LNvs under long day conditions.

Discussion

The experiments described above lead to two unexpected findings regarding the network properties of circadian entrainment in *Drosophila*. First, the l-LNvs govern the phase of evening peak of activity through PdfR dependent effects on evening cells that bypass the s-LNvs. Though previous work has implicated the l-LNvs in the control of evening peak phase (e.g., (Cusumano et al., 2009; Potdar and Sheeba, 2012)), our results are the first to provide evidence that there is a direct connection between the l-LNvs and evening cells within the AMe and that this connection mediates the photoperiodic adjustment of sleep and activity in the fly. Second, the HB-eyelets light input pathways, long-implicated in circadian entrainment, have opposing effects on the l-LNvs and s-LNvs, inhibiting the former and exciting the latter. These results reveal not only a differential effect of a light input pathway on specific nodes of the CCNN, but also establish that light from extraretinal photoreceptors can have synergistic or antagonistic effects on CRY- and compound eye-mediated light responses, depending on the clock neuron target in question.

Both the l-LNvs and s-LNvs express the blue light circadian photoreceptor CRY, the expression of which renders neurons directly excitable by light entering the brain through the cuticle (Fogle et al., 2011). How such CRY mediated light input interacts with input from external photoreceptors is not well understood, though it is known that each system alone is sufficient for the entrainment of locomotor rhythms (Helfrich-Förster et al., 2001). Genetic evidence suggests that the HB-eyelets have relatively weak effects on circadian entrainment: flies with functional eyelets that lack compound eyes, ocelli and CRY entrain relatively poorly to LD cycles relative to flies with functional eyes or CRY (Rieger et al., 2003). The small phase responses of locomotor rhythms to HB-eyelet excitation further supports a relatively weak effect of the eyelet on free running locomotor rhythms.

The LNvs are critical nodes in the CCNN and are closely associated with input pathways linking the central brain to external photoreceptors (Helfrich-Förster et al., 2007). Work on the LNvs has provided evidence for a division of labor among the l-LNvs and s-LNvs: the l-LNvs

are wake promoting neurons that acutely govern arousal and sleep independently of the s-LNvs (Parisky et al. 2008; Chung et al. 2008; Shang et al., 2008; Sheeba et al., 2008) while the s-LNvs act as key coordinators of the CCNN to support robust circadian timekeeping (Helfrich-Förster, 1998; Grima et al., 2004; Shafer and Taghert, 2009; Sheeba et al., 2010). Anatomical and genetic evidence has long supported the notion that the dorsal projections of the s-LNvs represent the key connection between the LNvs and the remaining components of the CCNN (e.g., (Helfrich-Förster, 1998; Grima et al., 2004; Fernandez et al., 2008; Sivachenko et al., 2013; Petsakou et al., 2015)). However, a smaller body of work has suggested that the l-LNvs also contribute to the entrainment of sleep/activity rhythms under LD cycles (Shang et al., 2008; Shafer and Taghert, 2009; Sheeba et al., 2010). Our Pdf knockdown and PdfR rescue experiments under long day conditions indicate that as the day grows longer the l-LNvs play a greater role in the timing of the evening peak (Fig. 3; compared to (Shafer and Taghert, 2009)). Moreover, the effects of PDF released from the l-LNvs are mediated not by the PDF receptive s-LNvs but rather by the 5th s-LNvs and a subset of the LNds (Fig. 5), the NPF and ITP co-expressing LNds in particular (with some influence of the other PDF-receptor positive LNds). These same neurons were recently identified as evening cells that are physiologically responsive to PDF but relatively weakly coupled to LNv clocks under conditions of constant darkness (Yao and Shafer, 2014). Our results suggest that the l-LNvs differentially modulate the NPF/ITP positive evening oscillators as a function of day length, producing stronger PDF dependent delays under long day conditions through increased release of PDF from the l-LNvs, thereby delaying the evening activity peak. Thus, the l-LNvs mediate their effects on the evening peak of activity through their action on the NPF/ITP positive subset of evening oscillators. The proposed PDF release from the l-LNvs under long days requires their activation via CRY and/or the compound eyes via ACh release from lamina L2 interneurons (Muraro and Ceriani, 2015). We hypothesize that the inhibitory influence of the H-B eyelets ceases under long days allowing the compound eyes and CRY to maximally excite the l-LNvs. Indeed, previous work has established that the compound eyes are especially important for adapting fly evening

activity to long days (Rieger et al., 2003). Furthermore, several studies have suggested that the compound eyes signal to the l-LNvs leading to enhanced PDF release and a slowing-down of the evening oscillators (Rieger et al., 2006; Wülbeck et al., 2009; Yoshii et al., 2009; Helfrich-Förster, 2014). A recent paper measuring Ca^{2+} rhythms in the different clock neurons *in vivo* supports this view (Liang et al., 2016): Ca^{2+} rhythms in the l-LNvs peak in the middle of the day, unlike the s-LNvs, which display Ca^{2+} peaks in the late night/early morning. We suggest that this phasing is produced by the inhibition of l-LNvs by the eyelets in the morning, followed by the excitation of the l-LNvs by the compound eyes and CRY. Interestingly, the only other clock neuron classes to display Ca^{2+} increases during the day are the LNds and 5^{th}-sLNv which phase lag the l-LNvs by approximately 2.5h and display peak Ca^{2+} levels in the late afternoon, a time that coincides with the evening peak of activity (Liang et al., 2016). We propose that the relative coordination of Ca^{2+} rhythms between the l-LNvs and the LNds/5^{th}-sLNv is produced by the connection we have identified between these neurons and the action of the eyelet and visual system on the l-LNvs (Figure 6).

Recent work has revealed that evening activity is promoted directly by the evening oscillator neurons and that the mid-day siesta is produced by the daily inhibition of evening oscillators by a group of dorsal clock neurons (Guo et al. 2016). We propose that the connections we have described here govern the timing of the evening peak of activity through the PDF dependent modulation of the molecular clocks within the evening oscillator neurons (Li et al. 2014; red arrows in Figure 6), though PDF modulation likely results in the excitation of target neurons (Seluzicki et al. 2014), which would promote evening activity. Our results reveal new and unexpected network properties underlying the entrainment of the circadian clock neuron network to LD cycles (summarized in Fig. 6). Excitatory effects of light on the LNvs are differentially modulated by the HB-eyelets via cholinergic excitation of the s-LNvs and histaminergic inhibition of the l-LNvs. Our work further reveals PDF dependent modulatory connections in the AMe between the l-LNvs and the s-LNvs and, most surprisingly, between the l-LNvs and a small subset of evening oscillators. Our work indicates that the latter connection is critical for the adjustment of evening activity phase during long, summer-like

days. This network model of entrainment reveals not only how CRY and external photoreceptors interact within specific nodes of the CCNN, but also how photoreception is likely to drive changes in CCNN output in the face of changing day-length.

Figure Legends

Figure 1: The HB-eyelet likely forms synapses directly on the LNv clock neurons within the accessory medulla and along its ventral elongation. (A-F) The *Rh6-GAL4* expression pattern (green) co-labeled with anti-PDF (magenta). (A) One hemisphere of a *UAS-GFP/+;Rh6-GAL4/+* brain co-immunolabeled for GFP and PDF. The axons of the Rh6 positive R8 photoreceptors of the compound eye cross the lamina (La) and terminate in the medulla (Me) whereas the axons of the HB-eyelet (asterisk) directly innervate the accessory medulla (AMe). Scale bar = 100µm. (B) Axonal terminals of the R8 photoreceptors (green) in the Me reside in close vicinity to the PDF positive puncta of the l-LNvs (magenta). Scale bar = 15µm. (C-F) Axons of the H-B-eyelet terminate in the AMe and overlap with PDF arborizations (magenta in (D) and (F)). Micrographs in C-F represent 20 µm projections of the AMe consisting of 10 optical sections separated by 2 µm steps. *Rh6-GAL4* is not expressed in the PDF neurons as no co-localization is visible in the cell bodies of the PDF neurons. For (C-F), scale bars = 15 µm. (C) and (D) and (E) and (F) display two different brains. (G-I) Reconstitution of GFP between LNv neurons and the Rh6-positive photoreceptors. (G) GFP fluorescence in a *Pdf-lexA/+;Rh6-GAL4/+* parental control. (H) GFP fluorescence in a *Pdf-lexA/lexAop-CD4::spGFP11;Rh6-GAL4/UAS-CD4::spGFP1-10* brain reveals GFP reconstitution within the AMe and along its ventral elongation. (I) GFP fluorescence in a *LexAop-CD4::spGFP11/+;UAS-CD4::spGFP1-10/+* parental control. (J-L) reconstituted GFP (green in (J) and (K)) in a *Pdf-lexA/lexAop-CD4::spGFP11;Rh6-GAL4/ UAS-CD4::spGFP1-10* brain co-labeled for PDF (magenta in (K) and (L). For (G-L), scale bars = 25µm. The arrows in panels (C), (E), (K), and (L) indicate the central part of the AMe, which is strongly innervated by H-B eyelet terminals in all brains. The asterisk in (A) indicates the HB-eyelet. The asterisks in (C), (E), and (K) indicate the ventral elongation of the AMe.

Figure 2: The s-LNvs but not the l-LNvs respond to HB-eyelet excitation with increases in calcium and cAMP. (A) P2X2 mediated excitation of HB-eyelets. Top two traces: average

563 GCaMP3.0 fluorescence plots (±SEM) for HB-eyelet nerves co-expressing P2X2 and
564 GCAMP in *Rh6-GAL4/UAS-GCaMP3.0;UAS-P2X2/+* brains in response to 30s perfusion of
565 1mM ATP (top trace, N=24) or vehicle (bottom trace, N=24). Histogram: comparison of
566 average maximum GCaMP responses (±SEM) for the same data. ATP caused significant
567 GCaMP fluorescence increases compared to vehicle control. (B). Effect of eyelet excitation
568 on l-LNv Ca^{2+} in *Pdf-lexA,LexA-GCaMP3.0/Rh6-GAL4; UAS-P2X2/+* brains in which P2X2 is
569 expressed in the HB-eyelet and GCaMP in the LNvs. Data arranged as in (A); N=14 for ATP
570 and N=15 for vehicle. The l-LNvs did not display significant GCaMP fluorescence increases
571 in response to eyelet excitation. (C) Effect of eyelet excitation on s-LNv Ca^{2+} in *Pdf-*
572 *lexA,LexAop-GCaMP3.0/Rh6-GAL4;UAS-P2X2/+* brains. Data arranged as in (A). N=20 for
573 ATP, N=13 for vehicle. Excitation of the eyelet resulted in significant GCaMP fluorescence
574 increases relative to vehicle controls. (D) In brains lacking a driver for UAS-P2X2 expression
575 in the eyelets (*Pdf-lexA,LexAop-GCaMP3.0/+;UAS-P2X2/+*). ATP failed to result in an
576 increase in s-LNv GCaMP fluorescence relative to vehicle controls. Data arranged as for (A).
577 N=13 for ATP, N= 13 for vehicle. For (A-D), scale bars represent 1 minute (x axis) and a 50%
578 change in GCaMP3.0 fluorescence over baseline (y-axis). (E) Effect of eyelet excitation on l-
579 LNv cAMP in *Pdf-lexA,LexAop-Epac1-camps/Rh6-GAL4;UAS-P2X2* brains. The two traces
580 display average inverse Epac1-camps FRET (CFP/YFP) plots for l-LNvs in response to 1
581 mM ATP (top trace, N=17) and vehicle (bottom trace, N=17). Histogram: comparison of
582 average maximum Epac1camps responses (±SEM) for the same data. ATP perfusion failed
583 to produce significant inverse FRET increases in l-LNvs relative to vehicle controls. (F)
584 Excitation of the eyelet causes cAMP increases in the s-LNvs of *Pdf-lexA,LexAop-Epac1-*
585 *camps/Rh6-GAL4;UAS-P2X2*. Data arranged as for (E). ATP produced significant inverse
586 FRET increases in the s-LNvs relative to vehicle controls. N=15 for ATP, N=14 for vehicle
587 (G) Average inverse Epac1-camps FRET (CFP/YFP) plots for l-LNvs in *Pdf-lexA,LexAop-*
588 *Epac1-camps/+;UAS-P2X2/+* brains that express Epac1-camps in the LNvs but fail to drive
589 P2X2 in the eyelet. The l-LNvs did not display inverse FRET increases in response to ATP
590 (middle plot, N=14) relative to vehicle controls (bottom plot, N=14). The l-LNvs did display

591 inverse FRET increases to 10-4 M nicotine (top plot, N=12). Histogram: comparison of
592 maximum Epac1-camps responses for the same data. ATP perfusion failed to produce
593 significant increases in CYP/YPF ratio in the l-LNvs relative to vehicle controls while nicotine
594 (10-4 M) produced significant cAMP increases. (H) Average inverse Epac1-camps FRET
595 (CFP/YFP) plots for s-LNvs in *Pdf-lexA,LexAop-Epac1-camps/+;UAS-P2X2/+* brains. Data
596 organized as for (G). ATP perfusion (N=19) caused small but significant increases CYP/YPF
597 ratio relative to vehicle controls (N=19) in the s-LNvs while nicotine (10-4 M, N=15) produced
598 large and significant inverse FRET increases. For (E-H), scale bars represent 1 minute (x-
599 axis) and a 25% changes in CFP/YFP ratio (y-axis). Bars under averaged plots represent 30
600 seconds of ATP perfusion switched from a constant saline flow. For all statistical
601 comparisons: n.s. (not significant) indicates $p \geq 0.05$, * indicates $p < 0.05$, ** indicates $p < 0.01$,
602 and *** indicates $p < 0.001$. (I) Response of a representative l-LNv to local pressure injection
603 of 100mM histamine (HA) into the ipsilateral Me. Black bars indicate stimulus length (0.5 s, 1
604 s, 10 s). Duration dependent inhibition of ipsilateral spiking activity (large spikes) was
605 apparent while contralateral activity (small spikes) was not affected. (J) Enlargements of the
606 boxed regions in I showing the inhibition after drug application. Note that spiking stops
607 abruptly but comes back gradually before returning to previous levels. mp, membrane
608 potential.

609

610 Figure 3: PDF is required specifically in the l-LNvs for normally phased evening peaks under
611 long day conditions. (A) The averaged activity profile of a *UAS-PdfRNAi* control fly under
612 LDR 16:8. The morning and evening peaks are aligned with dawn and dusk (light grey
613 regions of the LD cycle above the plot). (B) Activity of flies in which PDF has been knocked
614 down in all LNvs through the co-expression of *UAS-PdfRNAi* and *UAS-Dicer2* (Dcr2) under
615 the control of *Pdf-GAL4*. (C) Activity of flies in which PDF has been knocked down only in the
616 l-LNvs using the *c929-GAL4* driver (D). Activity of flies in which PDF has been knocked down
617 only in the s-LNvs using the *r6-GAL4* driver. (E) The average evening peak phase of flies in

which *Pdf* expression has been knocked down in different subsets of neurons. Knockdown of *Pdf* either in all LNvs or specifically in the l-LNvs, using *Pdf-GAL4* and *c929-GAL4*, respectively, resulted in a significantly advanced evening peak of activity compared to *Dicer2* over-expression and *UAS-PdfRNAi* controls. Knockdown of *Pdf* specifically in the s-LNvs using *R6-GAL4* failed to produce an advanced evening peak relative to controls. ANOVA followed by a post-hoc test revealed no significant differences in phase between *Dcr2;PdfG4, PdfRNAi, Dcr2/c929G4, Dcr2/r6G4* and *Dcr2/r6G4/PdfRNAi* flies ($p > 0.1199$). However, *Dcr2/PdfG4/PdfRNAi* and *Dcr2/c929G4/PdfRNAi* flies had a significant earlier evening peak than all others ($p < 0.001$). In addition, the evening peak phase between these two lines was significantly different ($p < 0.001$). (F) The average evening peak phase under LDR 16:8 of flies in which the LNvs have been electrically silenced (bottom row: *Pdf-GAL4/UAS-Kir2.1*). As expected these flies display an abnormally early evening peak of activity compared to *Pdf-GAL4* (top row) and *UAS-Kir2.1* (middle row) controls (Kruskal-Wallis test, $p < 0.001$). For (A-F), the numbers on the right side of the panels indicate sample size (G) PDF expression in a representative *UAS-Dicer2/c929-GAL4/UAS-PdfRNAi* brain. Only s-LNv PDF is visible. (H) PDF expression in a *UAS-Dicer2/R6-GAL4/UAS-PdfRNAi* brain. Only l-LNv PDF is visible. For (G) and (H) scale bars represent 20μm. In these experiments the *GAL4* and *UAS* elements were always present as single copies. The *GAL4* elements and *UAS-RNAi* elements were autosomal while the *UAS-Dcr2* element was inserted into the X chromosome. Thus, flies were heterozygous for *GAL4* and *UAS-RNAi* and hemizygous for the *UAS-Dicer2* element.

Figure 4: The l-LNvs modulate cAMP levels in the s-LNvs. (A) Averaged Epac1-camps inverse FRET plot (±SEM) of l-LNvs imaged in *c929-Gal4/Pdf-LexA,LexAop-Epac1-camps;UAS-P2X2/+* brains, before, during and after 30s perfusion of 1mM ATP (indicated on the bottom plot in each column). ATP/P2X2 mediated excitation caused clear inverse FRET increases. (B) Averaged Epac1-camps inverse FRET plot (±SEM) of s-LNvs from the same

645 brains as (A). Excitation of the *c929* network produced inverse FRET increases in the s-
646 LNvs. (C) Averaged Epac1-camps inverse FRET plot (±SEM) of large LNvs imaged in a *Pdfr*
647 mutant background using *han^{5304};c929-GAL4/Pdf-LexA,LexAop-Epac1-camps;UAS-P2X2/+*
648 brains. *c929* network excitation caused clear inverse FRET increases in these neurons. (D)
649 Averaged Epac1-camps plot (±SEM) of s-LNvs from the same brains as (C). Excitation of the
650 *c929* network failed to produce inverse FRET increases in the s-LNvs in the absence of PdfR
651 function. (E) Averaged Epac1-camps inverse FRET plot (±SEM) of large LNvs imaged in *Pdf-*
652 *LexA,LexAop-Epac1-camps/+;UAS-P2X2/+* brains. ATP failed to produce inverse FRET
653 increases in the absence of the GAL4 driver. The scale bars represent 60s (x-axis) and a
654 20% change in inverse FRET (y-axis) and also apply to (A) and (C). (F) Averaged Epac1-
655 camps inverse FRET plot (±SEM) of s-LNvs from the same brains as (E). ATP caused no
656 obvious inverse FRET increases. The scale bars in (F) represent 60s (x-axis) and a 10%
657 change in inverse FRET (y-axis) and also apply to (B) and (D). (G) Comparison of maximum
658 Epac1-camps responses for the l-LNv data shown in (A), (C), and (E). ATP (1mM) perfusion
659 caused significant inverse FRET increases in both the experimental ("exp" *c929-GAL4/Pdf-*
660 *LexA,LexAop-Epac1-camps;UAS-P2X2/+* and PdfR mutant ("-pdfr" *han^{5304};c929-GAL4/Pdf-*
661 *LexA,LexAop-Epac1-camps;UAS-P2X2/+* conditions, relative to the negative control lacking
662 the GAL4 driver for P2X2 expression ("-p2x2" *Pdf-LexA,LexAop-Epac1-camps/+;UAS-*
663 *P2X2/+*). (H) Comparison of maximum Epac1-camps responses for the s-LNv data shown in
664 (B), (D), and (F). ATP (1mM) perfusion caused significant inverse FRET increases in
665 experimental (exp) flies relative to both PdfR mutants (-pdfr) and –p2x2 controls. Genotypes
666 were identical to those in (G). For (G) and (H) *** indicates $p<0.001$ and n.s. indicates no
667 significant difference ($p\geq0.05$).

668

669 Figure 5: PdfR expression in a small group of evening cells is sufficient for normal evening
670 peak phase under long days. (A) The averaged activity profile of *han^{5304};UAS-Pdfr* control
671 flies under LDR 16:8. The evening peak is advanced compared to wild-type controls

(compare to Fig. 4c). (B) The averaged activity profile of *han^{5304};Pdf-GAL4/UAS-Pdfr* flies. *Pdfr* expression in the l- and s-LNvs is not sufficient to rescue normal evening peak phase. (C) The averaged activity profile of *han^{5304};Cry-GAL4/UAS-Pdfr* flies. The rescue of *Pdfr* expression in the *cry*- expressing clock neurons is sufficient to rescue normal evening peak phase. (D) The averaged activity profile of *han^{5304};UAS-Pdfr/+;R78G02-GAL4/+* flies. *Pdfr* expression in the *R78G02-GAL4* expressing neurons is sufficient to rescue normal evening peak phase. (E) The averaged activity profile of *han^{5304};npf-GAL4/UAS-Pdfr* flies. *Pdfr* expression in the NPF expressing clock neurons is sufficient to rescue normal evening peak phase. (F) A comparison of evening peak phases between, wild-type (WT) flies, flies lacking functional Pdfr (*PdfR-/UAS-PdfR*), and flies in which *Pdfr* expression has been rescued in various subsets of clock neurons using various GAL4 (G4) drivers. Only rescues that included the 5th s-LNv and CRY- positive LNds (bottom five genotypes) resulted in rescue of evening peak under LDR 16:8. ANOVA followed by a post-hoc test revealed highly significant differences in evening peak phase between the fly lines marked by asterisks and the ones without asterisks ($p < 0.001$). The lines with asterisks were not significantly different from each other ($p = 1.000$). Neither were the unmarked lines significantly different from each other ($p > 0.838$). (G) PDF (cyan) and CRY (magenta) expression in a single hemisphere of a *UAS-StingerGFP/+; R78G02-GAL4/+ brain*. Only the region bordering the central brain and Me is shown. (H) The same brain region as in (G) co-immunolabeled for GFP (green) and CRY (magenta). *R78G02-GAL4* drives GFP expression in the CRY-positive LNds and the 5th s-LNv. Another, non-clock neuron expressing GFP (asterisk) is also present in this brain region. (I) A GRASP brain preparation in which GFP (green) has been reconstituted between LNvs (magenta) and *R78G02-GAL4* expressing neurons. Reconstituted GFP is visible in the AMe near the s-LNvs. (J) A GRASP brain preparation as in (I). Reconstituted GFP is visible along dorsal projection (dp) of the s-LNvs. pot = posterior optic tract of the l-LNvs. For (G-I) scale bars = 20μm.

Figure 6: Network model of light input in the circadian clock neuron network that governs bimodal locomotor rhythms. The l-LNvs receive excitatory cholinergic from the compound eyes (ACh) and inhibitory histaminergic (His) input from the HB-eyelets while the s-LNvs receive excitatory ACh input from the HB-eyelets. Thus HB-eyelet activity antagonizes compound eye- and CRY-mediated light excitation in the l-LNvs while synergizing CRY-mediated excitation in the s-LNvs. Note: though we separate ACh and His terminals for the eyelet in the model, we do not mean to suggest that these two transmitters are differentially trafficked to different presynaptic termini. Rather, the differential effects of eyelet excitation are most likely due to the differential expression of receptors on the l-LNvs and s-LNvs. The l-LNvs modulate (red arrows) the s-LNvs and the E1 and E2 evening neurons via PDF. Such modulatory signaling likely sets the phase of the molecular clocks in target neurons, though it results in a modest excitation of targets as well (see discussion). We hypothesize that the effects of the H-B eyelets wane over the course of the day. Consequently, the excitatory influence of the compound eyes on the l-LNvs prevails under long days. The neuropeptides expressed by the various classes of clock neurons are indicated by color as is the pattern of CRY expression (dark blue outline). For the exception of the l-LNvs, PdfR is expressed wherever CRY is expressed. M: Morning neurons (s-LNv); E3: evening neurons that are not receptive to PDF.

Author Contributions

M.S., P.M., and E.D.B. conducted behavioral experiments. K.R.L., Z.Y., and J.D. conducted live imaging experiments. E.B. conducted the electrophysiological experiments. A.B. created the summary illustration. C. H-F., J.J.L.H., E.B., and O.T.S. designed the study. O.T.S. wrote the paper with help from the other authors.

Acknowledgements

This work was supported by NIH (NINDS) grants R00NS062953 and R01NS077933 to O. T. S., the German Research Foundation grants DFG; Fo207/10-3 and SFB1047, INST 93/784-1 and the European Community 6th Framework Project EUCLOCK no. 018741 to C.H-F., and a BBSRC grant BB/J0127221/1 to J.J.L.H. M.S. was further sponsored by a Hanns-Seidel-Foundation excellence grant funded by the BMBF (German Ministry for Education and Research). We thank J. Park, P. Emery, P. Hardin F. Rouyer, P. Taghert and N. Glossop for sharing fly strains and P. Hardin, D. Nässel, H. Dircksen, and T. Todo for providing antisera. Finally, we wish to acknowledge T. Yoshii, and C. Hermann-Luibl for their characterization of the *R78G02-GAL4* line and Kate Abruzzi and Michael Rosbash for helpful comments on the manuscript.

735 **References:**

736 Aschoff J (1981a) Biological Rhythms. New York: Plenum Press.

737 Aschoff J (1981b) Freerunning and entrained circadian rhythms. In. New York: Plenum
738 Press.

739 Baines RA, Uhler JP, Thompson A, Sweeney ST, Bate M (2001) Altered electrical properties
740 in *Drosophila* neurons developing without synaptic transmission. J Neurosci 21:1523-
741 1531.

742 Barolo S, Carver LA, Posakony JW (2000) GFP and beta-galactosidase transformation
743 vectors for promoter/enhancer analysis in *Drosophila*. BioTechniques 29:726, 728,
744 730, 732.

745 Bernstein JG, Garrity PA, and Boyden ES (2012) Optogenetics and thermogenetics:
746 technologies for controlling the activity of targeted cells within intact neural circuits.
747 Curr Opin Neurobiol 22:61-71.

748 Burg MG, Sarthy PV, Koliantz G, Pak WL (1993) Genetic and molecular identification of a
749 *Drosophila histidine decarboxylase* gene required in photoreceptor transmitter
750 synthesis. EMBO J 12:911-919.

751 Cao G, Nitabach MN (2008) Circadian control of membrane excitability in *Drosophila*
752 *melanogaster* lateral ventral clock neurons. J Neurosci 28:6493-6501.

753 Chen C, Buhl E, Xu M, Croset V, Rees JS, Lilley KS, Benton R, Hodge JJ, Stanewsky R.
754 (2015) Drosophila Ionotropic Receptor 25a mediates circadian clock resetting by
755 temperature. Nature 527:516-20.

756 Chung BY, Kilman VL, Keath JR, Pitman JL, and Allada R. (2009) The GABAA Receptor
757 RDL Acts in Peptidergic PDF Neurons to Promote Sleep in Drosophila. Current
758 Biology 19: 386-390.

759 Cusumano P, Klarsfeld A, Chelot E, Picot M, Richier B, Rouyer F (2009) PDF-modulated
760 visual inputs and cryptochrome define diurnal behavior in *Drosophila*. Nat Neurosci
761 12:1431-1437.

762 Czeisler CA, Duffy JF, Shanahan TL, Brown EN, Mitchell JF, Rimmer DW, Ronda JM, Silva
763 EJ, Allan JS, Emens JS, Dijk DJ, Kronauer RE (1999) Stability, precision, and near-
764 24-hour period of the human circadian pacemaker. Science 284:2177-2181.
765 Diez-Noguera A (2013) Methods for serial analysis of long time series in the study of
766 biological rhythms. Journal of circadian rhythms 11:7.
767 Eck S, Helfrich-Förster C, and Rieger D (2016) The Timed Depolarization of Morning and
768 Evening Oscillators Phase Shifts the Circadian Clock of Drosophila. Journal of
769 Biological Rhythms, *In Press.*
770 Feinberg EH, Vanhoven MK, Bendesky A, Wang G, Fetter RD, Shen K, Bargmann CI (2008)
771 GFP Reconstitution Across Synaptic Partners (GRASP) defines cell contacts and
772 synapses in living nervous systems. Neuron 57:353-363.
773 Fernandez MP, Berni J, Ceriani MF (2008) Circadian remodeling of neuronal circuits involved
774 in rhythmic behavior. PLoS Biol 6:e69.
775 Fogle KJ, Parson KG, Dahm NA, Holmes TC (2011) CRYPTOCHROME is a blue-light
776 sensor that regulates neuronal firing rate. Science 331:1409-1413.
777 Glossop NR, Houl JH, Zheng H, Ng FS, Dudek SM, Hardin PE (2003) VRILLE feeds back to
778 control circadian transcription of Clock in the *Drosophila* circadian oscillator. Neuron
779 37:249-261.
780 Golombek DA, Rosenstein RE (2010) Physiology of circadian entrainment. Physiol Rev
781 90:1063-1102.
782 Gordon MD, Scott K (2009) Motor control in a *Drosophila* taste circuit. Neuron 61:373-384.
783 Grima B, Chelot E, Xia R, Rouyer F (2004) Morning and evening peaks of activity rely on
784 different clock neurons of the *Drosophila* brain. Nature 431:869-873.
785 Gummadova JO, Coutts GA, Glossop NR (2009) Analysis of the *Drosophila Clock* promoter
786 reveals heterogeneity in expression between subgroups of central oscillator cells and
787 identifies a novel enhancer region. J Biol Rhythms 24:353-367.
788 Guo F, Cerullo I, Chen X, Rosbash M (2014) PDF neuron firing phase-shifts key circadian
789 activity neurons in *Drosophila*. Elife 3.

790 Guo F, Yu J, Jung HJ, Abruzzi KC, Luo W, Griffith LC, and Rosbash M (2016) Circadian
791 Neuron Feedback Controls the Drosophila Sleep-Activity Profile. Nature, *In Press*.

792 Hamada FN, Rosenzweig M, Kang K, Pulver SR, Ghezzi A, Jegla TJ, Garrity PA (2008) An
793 internal thermal sensor controlling temperature preference in *Drosophila*. Nature
794 454:217-220.

795 Hamasaka Y and Nässel DR (2006) Mapping of serotonin, dopamine, and histamine in
796 relation to different clock neurons in the brain of Drosophila. Journal of Comparative
797 Neurology 494:314-330.

798 Helfrich-Förster C (1997) Development of pigment-dispersing hormone-immunoreactive
799 neurons in the nervous system of *Drosophila melanogaster*. JCompNeurol 380:335-
800 354.

801 Helfrich-Förster C (1998) Robust circadian rhythmicity of *Drosophila melanogaster* requires
802 the presence of lateral neurons: a brain-behavioral study of disconnected mutants. J
803 Comp Physiol [A] 182:435-453.

804 Helfrich-Förster C (2002) The circadian system of *Drosophila melanogaster* and its light input
805 pathways. Zoology (Jena) 105:297-312.

806 Helfrich-Förster C (2014) From neurogenetic studies in the fly brain to a concept in circadian
807 biology. J Neurogenet 28:329-347.

808 Helfrich-Förster C, Winter C, Hofbauer A, Hall JC, Stanewsky R (2001) The circadian clock of
809 fruit flies is blind after elimination of all known photoreceptors. Neuron 30:249-261.

810 Helfrich-Förster C, Edwards T, Yasuyama K, Wisotzki B, Schneuwly S, Stanewsky R,
811 Meinertzhagen IA, Hofbauer A (2002) The extraretinal eyelet of *Drosophila*:
812 development, ultrastructure, and putative circadian function. J Neurosci 22:9255-
813 9266.

814 Helfrich-Förster C, Yoshii T, Wülbeck C, Grieshaber E, Rieger D, Bachleitner W, Cusamano
815 P, Rouyer F (2007) The lateral and dorsal neurons of *Drosophila melanogaster*: new

816 insights about their morphology and function. Cold Spring Harb Symp Quant Biol
817 72:517-525.
818 Hermann-Luibl C, Yoshii T, Senthilan PR, Dircksen H, Helfrich-Förster C (2014) The ion
819 transport peptide is a new functional clock neuropeptide in the fruit fly *Drosophila*
820 *melanogaster*. J Neurosci 34:9522-9536.
821 Herzog ED (2007) Neurons and networks in daily rhythms. Nature reviews Neuroscience
822 8:790-802.
823 Hewes RS, Park D, Gauthier SA, Schaefer AM, Taghert PH.(2003) The bHLH protein
824 Dimmed controls neuroendocrine cell differentiation in Drosophila. Development
825 130:1771-1781
826 Hofbauer A, Buchner E (1989) Does *Drosophila* have seven eyes? Naturwissenschaften
827 76:335-336.
828 Hong ST, Bang S, Paik D, Kang J, Hwang S, Jeon K, Chun B, Hyun S, Lee Y, Kim J (2006)
829 Histamine and its receptors modulate temperature-preference behaviors in
830 *Drosophila*. J Neurosci 26:7245-7256.
831 Hyun S, Lee Y, Hong ST, Bang S, Paik D, Kang J, Shin J, Lee J, Jeon K, Hwang S, Bae E,
832 Kim J (2005) Drosophila GPCR *Han* is a receptor for the circadian clock neuropeptide
833 PDF. Neuron 48:267-278.
834 Im SH, Taghert PH (2010) PDF receptor expression reveals direct interactions between
835 circadian oscillators in *Drosophila*. J Comp Neurol 518:1925-1945.
836 Johard HA, Yoishii T, Dircksen H, Cusumano P, Rouyer F (2009) Peptidergic clock neurons
837 in *Drosophila*: ion transport peptide and short neuropeptide F in subsets of dorsal and
838 ventral lateral neurons. J Comp Neurol 516:59-73.
839 Lee G, Bahn JH, Park JH (2006) Sex- and clock-controlled expression of the neuropeptide F
840 gene in *Drosophila*. Proceedings of the National Academy of Sciences of the United
841 States of America 103:12580-12585.

842 Lelito KR, Shafer OT (2012) Reciprocal cholinergic and GABAergic modulation of the small
843 ventrolateral pacemaker neurons of *Drosophila's* circadian clock neuron network.
844 Journal of neurophysiology 107:2096-2108.
845 Li Y, Guo F, Shen J, Rosbash (2014) PDF and cAMP enhance PER stability
846 in Drosophila clock neurons. Proc. Natl. Acad. Sci. U S A. 111:E1284-1290.
847 Liang X, Holy TE, Taghert PH (2016) Synchronous *Drosophila* circadian pacemakers display
848 nonsynchronous Ca^{2+} rhythms in vivo. Science 351:976-981.
849 Lima SQ, Miesenböck G (2005) Remote control of behavior through genetically targeted
850 photostimulation of neurons. Cell 121:141-152.
851 Malpel S, Klarsfeld A, Rouyer F (2002) Larval optic nerve and adult extra-retinal
852 photoreceptors sequentially associate with clock neurons during *Drosophila* brain
853 development. Development 129:1443-1453.
854 McCarthy EV, Wu Y, Decarvalho T, Brandt C, Cao G, Nitabach MN (2011) Synchronized
855 bilateral synaptic inputs to *Drosophila melanogaster* neuropeptidergic rest/arousal
856 neurons. J Neurosci 31:8181-8193.
857 Menegazzi P, Vanin S, Yoshii T, Rieger D, Hermann C, Dusik V, Kyriacou CP, Helfrich-
858 Förster C, Costa R (2013) *Drosophila* clock neurons under natural conditions. J Biol
859 Rhythms 28:3-14.
860 Mertens I, Vandingenen A, Johnson EC, Shafer OT, Li W, Trigg JS, De Loof A, Schoofs L,
861 Taghert PH (2005) PDF receptor signaling in *Drosophila* contributes to both circadian
862 and geotactic behaviors. Neuron 48:213-219.
863 Münch M, Bromundt V (2012) Light and chronobiology: implications for health and disease.
864 Dialogues in clinical neuroscience 14:448-453.
865 Muraro NI, Ceriani MF (2015) Acetylcholine from Visual Circuits Modulates the Activity of
866 Arousal Neurons in *Drosophila*. J Neurosci 35:16315-16327.
867 Nitabach MN, Taghert PH (2008) Organization of the *Drosophila* circadian control circuit.
868 Curr Biol 18:R84-93.

869 Pantazis A, Segaran A, Liu CH, Nikolaev A, Rister J, Thum AS, Roeder T, Semenov E,
870 Juusola M, Hardie RC (2008) Distinct roles for two histamine receptors (hclA and
871 hclB) at the *Drosophila* photoreceptor synapse. J Neurosci 28:7250-7259.
872 Parisky KM, Agosto J, Pulver SR, Shang Y, Kuklin E, Hodge JJL, Kang K, Liu X, Garrity PA,
873 Rosbash M, and Griffith LC (2008) PDF Cells Are a GABA-Responsive Wake-
874 Promoting Component of the Drosophila Sleep Circuit. Neuron 60: 672-682
875 Petsakou A, Sapsis TP, Blau J (2015) Circadian Rhythms in *Rho1* Activity Regulate
876 Neuronal Plasticity and Network Hierarchy. Cell.
877 Picot M, Cusumano P, Klarsfeld A, Ueda R, Rouyer F (2007) Light activates output from
878 evening neurons and inhibits output from morning neurons in the *Drosophila* circadian
879 clock. PLoS Biol 5:e315.
880 Pittendrigh CS (1981) Circadian systems: entrainment. In: Handbook of behavioral
881 neurobiology (Aschoff J, ed), pp 95-124. New York: Plenum Press.
882 Pollack I, Hofbauer A (1991) Histamine-like immunoreactivity in the visual system and brain
883 of *Drosophila melanogaster*. Cell and tissue research 266:391-398.
884 Potdar S, Sheeba V (2012) Large ventral lateral neurons determine the phase of evening
885 activity peak across photoperiods in *Drosophila melanogaster*. J Biol Rhythms
886 27:267-279.
887 Renn SC, Park JH, Rosbash M, Hall JC, Taghert PH (1999) A *pdf* neuropeptide gene
888 mutation and ablation of PDF neurons each cause severe abnormalities of behavioral
889 circadian rhythms in *Drosophila*. Cell 99:791-802.
890 Rieger D, Stanewsky R, Helfrich-Förster C (2003) Cryptochrome, compound eyes, Hofbauer-
891 Buchner eyelets, and ocelli play different roles in the entrainment and masking
892 pathway of the locomotor activity rhythm in the fruit fly *Drosophila melanogaster*. J
893 Biol Rhythms 18:377-391.
894 Rieger D, Shafer OT, Tomioka K, Helfrich-Förster C (2006) Functional analysis of circadian
895 pacemaker neurons in *Drosophila melanogaster*. J Neurosci 26:2531-2543.

896 Roenneberg T, Merrow M (2003) The network of time: understanding the molecular circadian
897 system. Curr Biol 13:R198-207.
898 Ruben M, Drapeau MD, Mizrak D, Blau J (2012) A mechanism for circadian control of
899 pacemaker neuron excitability. J Biol Rhythms 27:353-364.
900 Schlichting M, Helfrich-Förster C (2015) Photic entrainment in *Drosophila* assessed by
901 locomotor activity recordings. Methods Enzymol 552:105-123.
902 Schmid B, Helfrich-Förster C, Yoshii T (2011) A new ImageJ plug-in "ActogramJ" for
903 chronobiological analyses. J Biol Rhythms 26:464-467.
904 Shafer OT, Taghert PH (2009) RNA-interference knockdown of *Drosophila* pigment
905 dispersing factor in neuronal subsets: the anatomical basis of a neuropeptide's
906 circadian functions. PloS one 4:e8298.
907 Shafer OT, Kim DJ, Dunbar-Yaffe R, Nikolaev VO, Lohse MJ, Taghert PH (2008)
908 Widespread receptivity to neuropeptide PDF throughout the neuronal circadian clock
909 network of *Drosophila* revealed by real-time cyclic AMP imaging. Neuron 58:223-237.
910 Shang Y, Griffith LC, Rosbash M (2008) Light-arousal and circadian photoreception circuits
911 intersect at the large PDF cells of the *Drosophila* brain. Proceedings of the National
912 Academy of Sciences of the United States of America 105:19587-19594.
913 Sheeba V, Fogle KJ, Holmes TC (2010) Persistence of morning anticipation behavior and
914 high amplitude morning startle response following functional loss of small ventral
915 lateral neurons in *Drosophila*. PloS one 5:e11628.
916 Sheeba V, Gu H, Sharma VK, O'Dowd DK, Holmes TC (2008) Circadian- and light-
917 dependent regulation of resting membrane potential and spontaneous action potential
918 firing of *Drosophila* circadian pacemaker neurons. Journal of neurophysiology 99:976-
919 988.
920 Siegmund T, Korge G (2001) Innervation of the ring gland of *Drosophila melanogaster*.
921 Comp Neurol 431:481-491.

922 Sivachenko A, Li Y, Abruzzi KC, Rosbash M (2013) The transcription factor *Mef2* links the
923 *Drosophila* core clock to *Fas2*, neuronal morphology, and circadian behavior. Neuron
924 79:281-292.
925 Sprecher SG, Desplan C (2008) Switch of rhodopsin expression in terminally differentiated
926 *Drosophila* sensory neurons. Nature 454:533-537.
927 Stewart BA, Atwood HL, Renger JJ, Wang J, Wu CF (1994) Improved stability of *Drosophila*
928 larval neuromuscular preparations in haemolymph-like physiological solutions.
929 Journal of comparative physiology A, Sensory, neural, and behavioral physiology
930 175:179-191.
931 Tian L, Hires SA, Mao T, Huber D, Chiappe ME, Chalasani SH, Petreanu L, Akerboom J,
932 McKinney SA, Schreiter ER, Bargmann CI, Jayaraman V, Svoboda K, Looger LL
933 (2009) Imaging neural activity in worms, flies and mice with improved GCaMP
934 calcium indicators. Nat Methods 6:875-881.
935 Veleri S, Rieger D, Helfrich-Förster C, Stanewsky R (2007) Hofbauer-Buchner eyelet affects
936 circadian photosensitivity and coordinates TIM and PER expression in *Drosophila*
937 clock neurons. J Biol Rhythms 22:29-42.
938 Viswanath V, Story GM, Peier AM, Petrus MJ, Lee VM, Hwang SW, Patapoutian A, and
939 Jegla T (2003) Opposite thermosensor in fruitfly and mouse. Nature 423:822-823.
940 Welsh DK, Takahashi JS, Kay SA (2010) Suprachiasmatic nucleus: cell autonomy and
941 network properties. Annu Rev Physiol 72:551-577.
942 Wülbeck C, Grieshaber E, Helfrich-Förster C (2009) Blocking endocytosis in *Drosophila's*
943 circadian pacemaker neurons interferes with the endogenous clock in a PDF-
944 dependent way. Chronobiology international 26:1307-1322.
945 Yao Z, Shafer OT (2014) The *Drosophila* circadian clock is a variably coupled network of
946 multiple peptidergic units. Science 343:1516-1520.
947 Yao Z, Macara AM, Lelito KR, Minosyan TY, Shafer OT (2012) Analysis of functional
948 neuronal connectivity in the *Drosophila* brain. Journal of neurophysiology 108:684-
949 696.

950 Yasuyama K, Meinertzhagen IA (1999) Extraretinal photoreceptors at the compound eye's
951 posterior margin in *Drosophila melanogaster*. J Comp Neurol 412:193-202.
952 Yasuyama K, Salvaterra PM (1999) Localization of choline acetyltransferase-expressing
953 neurons in *Drosophila* nervous system. Microscopy research and technique 45:65-79.
954 Yoshii T, Todo T, Wülbeck C, Stanewsky R, Helfrich-Förster C (2008) Cryptochrome is
955 present in the compound eyes and a subset of *Drosophila's* clock neurons. J Comp
956 Neurol 508:952-966.
957 Yoshii T, Wülbeck C, Sehadova H, Veleri S, Bichler D, Stanewsky R, Helfrich-Förster C
958 (2009) The neuropeptide pigment-dispersing factor adjusts period and phase of
959 *Drosophila's* clock. J Neurosci 29:2597-2610.
960 Zhang L, Chung BY, Lear BC, Kilman VL, Liu Y, Mahesh G, Meissner RA, Hardin PE, Allada
961 R (2010) DN1(p) circadian neurons coordinate acute light and PDF inputs to produce
962 robust daily behavior in *Drosophila*. Curr Biol 20:591-599.

963

964

965

966

967

968

969

970

971

972

973

974

975

976

Figure 1:

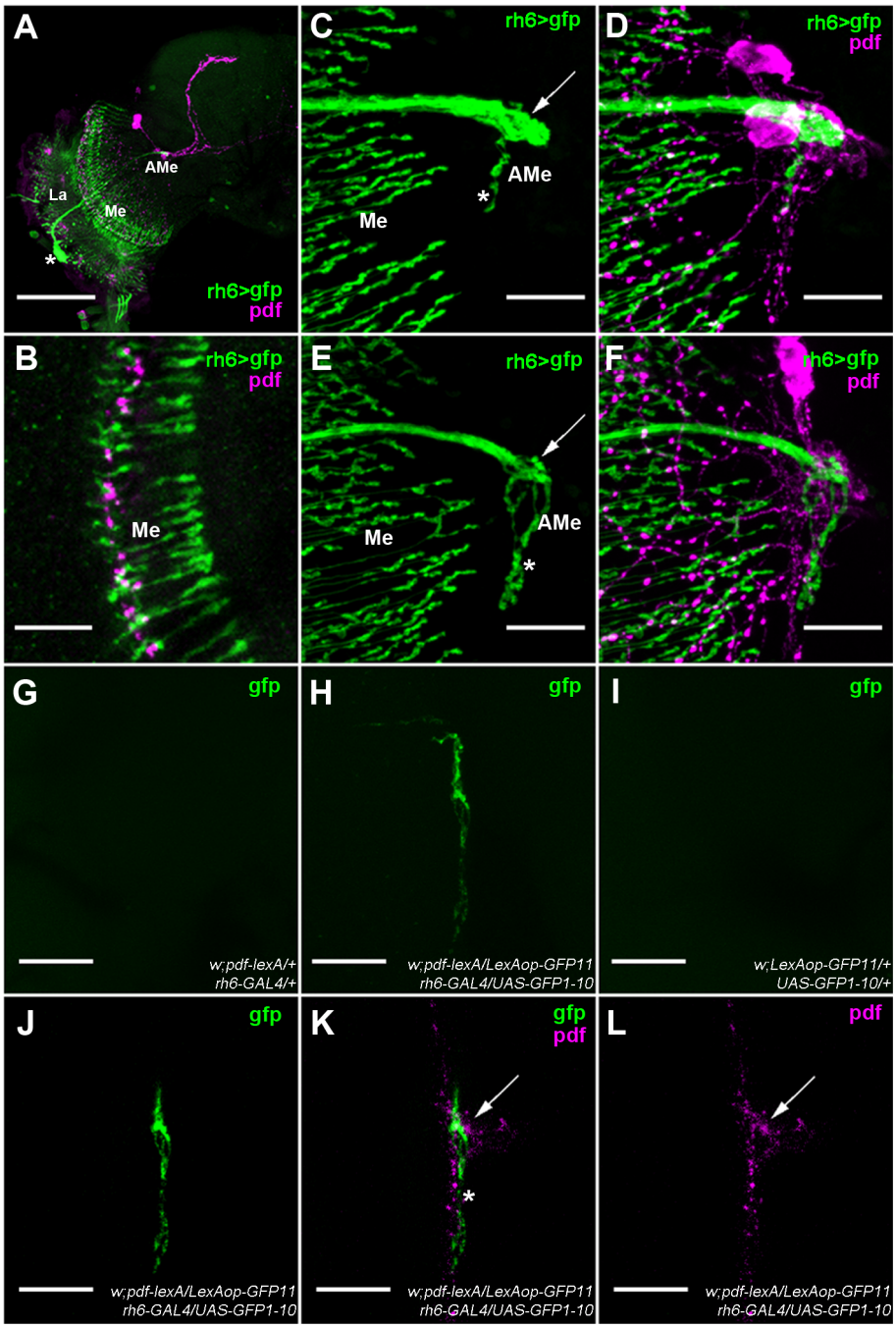
A
AMe
La
Me
*
rh6>gfp
pdf
C
rh6>gfp
AMe
*
Me
D
rh6>gfp
pdf
B
rh6>gfp
pdf
Me
E
rh6>gfp
Me
AMe
*
F
rh6>gfp
pdf
G
gfp
w;pdf-lexA/+
rh6-GAL4/+
H
gfp
w;pdf-lexA/LexAop-GFP11
rh6-GAL4/UAS-GFP1-10
I
gfp
w;LexAop-GFP11/+
UAS-GFP1-10/+
J
gfp
w;pdf-lexA/LexAop-GFP11
rh6-GAL4/UAS-GFP1-10
K
gfp
pdf
*
w;pdf-lexA/LexAop-GFP11
rh6-GAL4/UAS-GFP1-10
L
pdf
w;pdf-lexA/LexAop-GFP11
rh6-GAL4/UAS-GFP1-10

Figure 2:

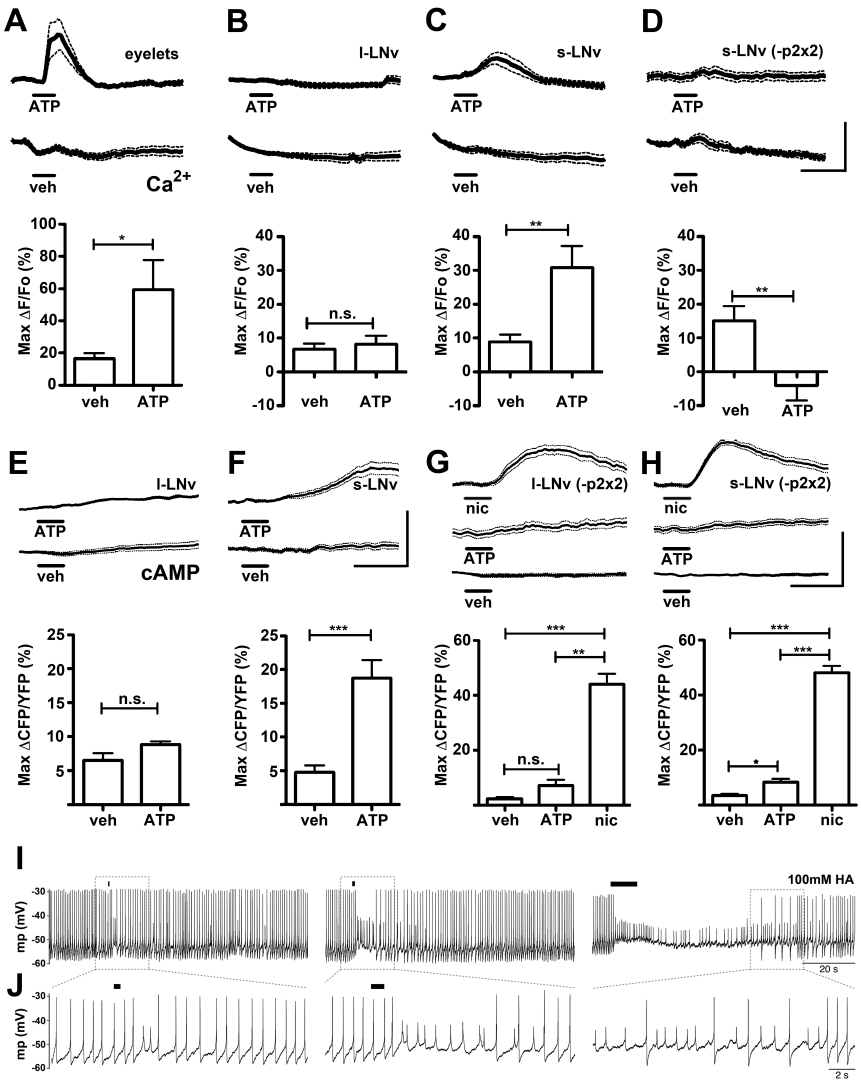
A
eyelets
ATP
veh
Ca2+
Max ΔF/Fo (%)
veh
ATP
B
l-LNv
n.s.
C
s-LNv
D
s-LNv (-p2x2)
E
cAMP
Max ΔCFP/YFP (%)
F
G
nic
H
I
100mM HA
mp (mV)
20 s
J
2 s

Figure 3:

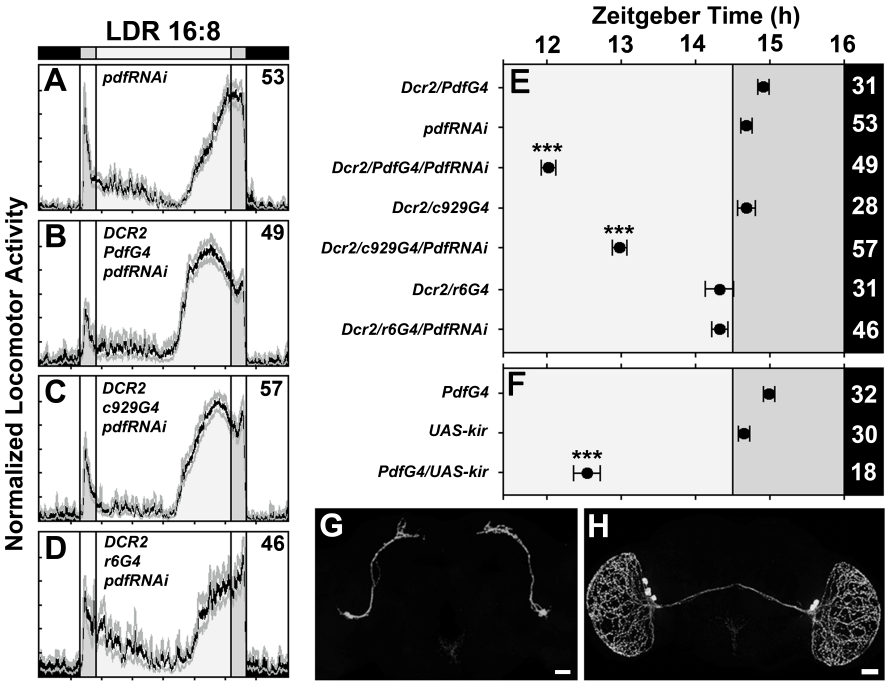
LDR 16:8
Normalized Locomotor Activity
A
pdfRNAi
53
B
DCR2
PdfG4
pdfRNAi
49
C
DCR2
c929G4
pdfRNAi
57
D
DCR2
r6G4
pdfRNAi
46
Zeitgeber Time (h)
12
13
14
15
16
E
Dcr2/PdfG4
31
pdfRNAi
53
***
Dcr2/PdfG4/PdfRNAi
49
Dcr2/c929G4
28
***
Dcr2/c929G4/PdfRNAi
57
Dcr2/r6G4
31
Dcr2/r6G4/PdfRNAi
46
F
PdfG4
32
UAS-kir
30
***
PdfG4/UAS-kir
18
G
H

Figure 4:

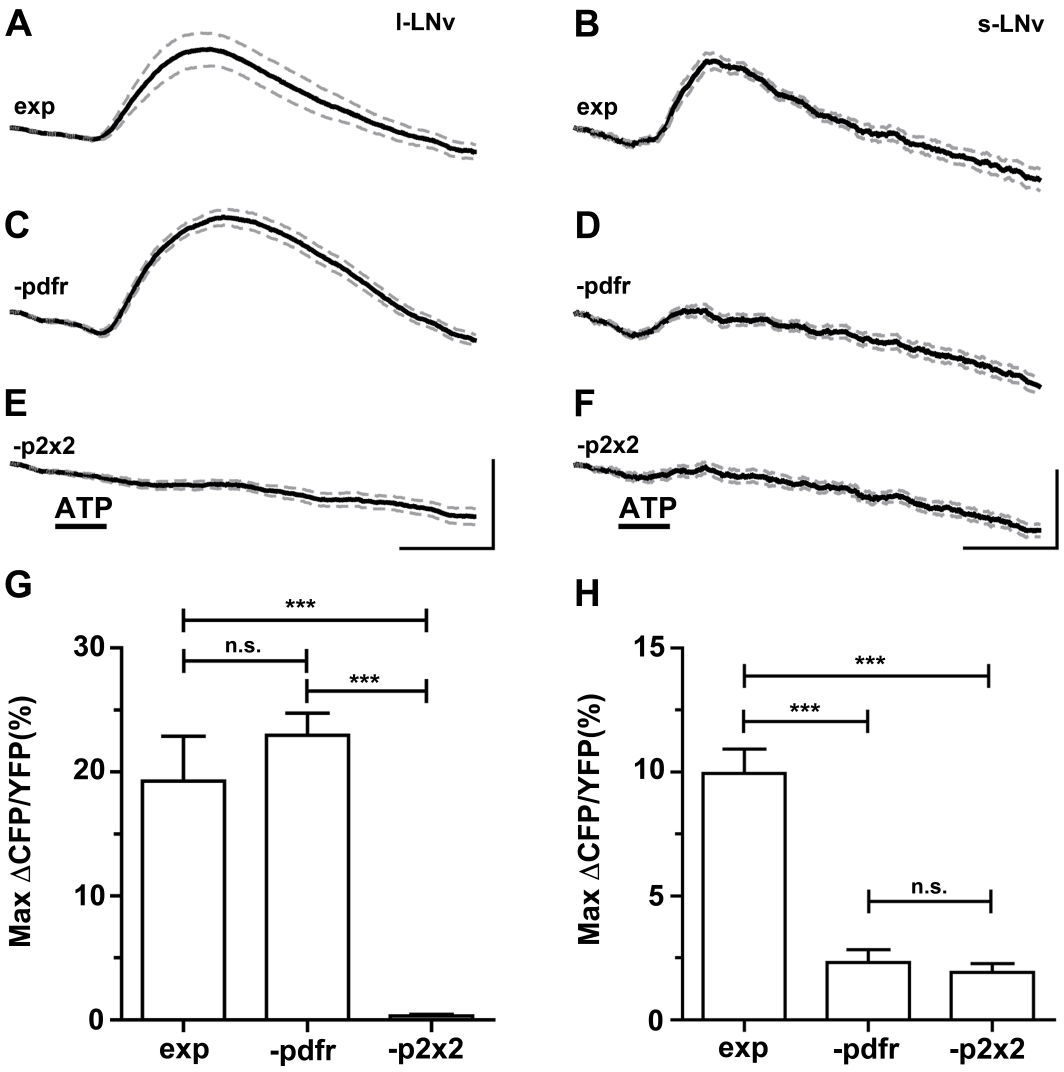
A
l-LNv
exp
B
s-LNv
exp
C
-pdfr
D
-pdfr
E
-p2x2
ATP
F
-p2x2
ATP
G
Max ΔCFP/YFP(%)
30
20
10
0
***
n.s.
***
exp
-pdfr
-p2x2
H
Max ΔCFP/YFP(%)
15
10
5
0
***
***
n.s.
exp
-pdfr
-p2x2

Figure 5:

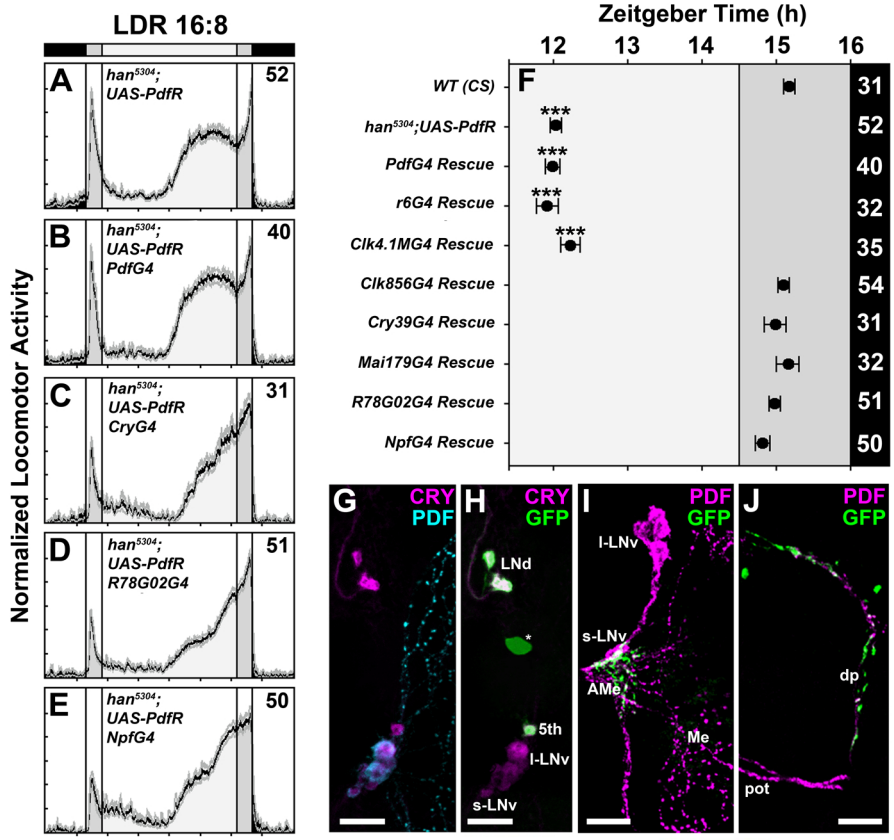
LDR 16:8
Normalized Locomotor Activity
A
han5304; UAS-PdfR
52
B
han5304; UAS-PdfR PdfG4
40
C
han5304; UAS-PdfR CryG4
31
D
han5304; UAS-PdfR R78G02G4
51
E
han5304; UAS-PdfR NpfG4
50
Zeitgeber Time (h)
12
13
14
15
16
F
WT (CS)
31
han5304;UAS-PdfR
52
PdfG4 Rescue
40
r6G4 Rescue
32
Clk4.1MG4 Rescue
35
Clk856G4 Rescue
54
Cry39G4 Rescue
31
Mai179G4 Rescue
32
R78G02G4 Rescue
51
NpfG4 Rescue
50
***
G
CRY
PDF
H
CRY
GFP
LNd
*
5th
l-LNv
s-LNv
I
PDF
GFP
l-LNv
s-LNv
AMe
Me
J
PDF
GFP
dp
pot

1042

1043 **Figure 6:**

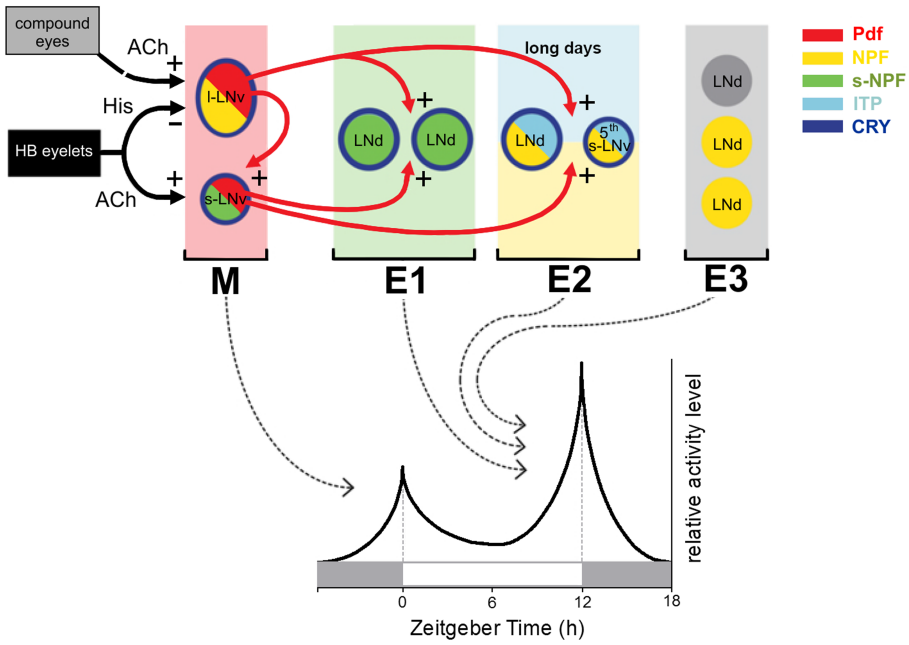

1044